Available online at www.sciencedirect.com
ScienceDirect
International Journal of Rock Mechanics & Mining Sciences 45 (2008) 689–700
International Journal of Rock Mechanics and Mining Sciences
www.elsevier.com/locate/ijrmms

Stability charts for rock slopes based on the Hoek–Brown failure criterion

A.J. Li[a,*], R.S. Merifield[a], A.V. Lyamin[b]

[a]Centre for Offshore Foundations Systems, The University of Western Australia, Perth, WA 6009, Australia
[b]Centre for Geotechnical and Materials Modelling, The University of Newcastle, NSW 2308, Australia

Received 20 April 2007; accepted 1 August 2007
Available online 17 October 2007

Abstract

This paper uses numerical limit analysis to produce stability charts for rock slopes. These charts have been produced using the most recent version of the Hoek–Brown failure criterion. The applicability of this criterion is suited to isotropic and homogeneous intact rock, or heavily jointed rock masses. The rigorous limit analysis results were found to bracket the true slope stability number to within $\pm 9\%$ or better, and the difference in safety factor between bound solutions and limit equilibrium analyses using the same Hoek–Brown failure criterion is less than 4%. The accuracy of using equivalent Mohr–Coulomb parameters to estimate the stability number has also been investigated. For steep slopes, it was found that using equivalent parameters produces poor estimates of safety factors and predictions of failure surface shapes. The reason for this lies in how these equivalent parameters are estimated, which is largely to do with estimating a suitable minor principal stress range. In order to obtain better equivalent parameter solutions, this paper proposes new equations for estimating the minor principal stress for steep and gentle slopes, which can be used to determine equivalent Mohr–Coulomb parameters.

Keywords: Safety factor; Limit analysis; Rock; Slope stability; Failure criterion

1. Introduction

Predicting the stability of rock slopes is a classical problem for geotechnical engineers and also plays an important role when designing for dams, roads, tunnels and other engineering structures. Many researchers have focused on assessing the stability of rock slope [1–3]. However, the problem of rock slopes still presents a significant challenge to designers.

Stability charts for soil slopes were first produced by Taylor [4] and they continue to be used extensively as design tools and draw the attention of many investigators [1,5]. Unfortunately, there are no such stability charts for rock slopes in the literature that are based on rock mass strength criteria. Although the stability charts proposed by Hoek and Bray [1] for Mohr–Coulomb material can be applied to rock or rockfill slopes, this requires knowledge of the equivalent Mohr–Coulomb cohesion and friction for the rock mass. Unfortunately, the strength of rock masses is notoriously difficult to assess. Nonetheless, many criteria have been proposed for estimating rock strength [6–10]. Currently, one widely accepted approach to estimating rock mass strength is the Hoek–Brown failure criterion [6,11]. However, since most geotechnical software uses the Mohr–Coulomb failure criterion, stability chart solutions based on the Hoek–Brown yield criterion do not appear in the literature.

Generally speaking, rock masses are inhomogeneous, discontinuous media composed of rock material and naturally occurring discontinuities such as joints, fractures and bedding planes. These features make any analysis very difficult using simple theoretical solutions, like the limit equilibrium method. Moreover, without including special interface or joint elements, the displacement finite element method is not suitable for analysing rock masses with fractures and discontinuities. Fortunately, the upper and lower bound formulations developed by Lyamin and Sloan

*Corresponding author. Tel.: +61 8 6488 3141; fax: +61 8 6488 1044.
E-mail addresses: anjui@civil.uwa.edu.au (A.J. Li), merifield@civil.uwa.edu.au (R.S. Merifield), andrei.lyamin@newcastle.edu.au (A.V. Lyamin).

1365-1609/$ - see front matter
doi:10.1016/j.ijrmms.2007.08.010

[12,13] and Krabbenhoft et al. [14] are ideally suited to modelling jointed or fissured materials because discontinuities exist inherently throughout the mesh. This feature was recently exploited by Sutcliffe et al. [15] and Merifield et al. [16] for predicting the bearing capacity of jointed rocks.

The purpose of this paper is to take advantage of the limit theorems ability to bracket the actual stability number of rock slopes. Both the upper and lower bounds are employed to provide this set of stability charts. These solutions are obtained from numerical techniques developed by Lyamin and Sloan [12,13] and Krabbenhoft et al. [14] where the well-known Hoek–Brown yield criterion has been incorporated into limit analysis as presented by Merifield et al. [16].

As a means of comparison, the limit equilibrium method will then be used in conjunction with equivalent Mohr–Coulomb parameters for the rock and compared with the solutions obtained from the numerical limit analysis approaches. This will allow the validity of using equivalent Mohr–Coulomb parameters for rock slope calculations to be investigated.

2. Previous studies

The stability of rock slopes has attracted the attention of researchers for decades. In order to deal with the complications of rock slope failure mechanisms, Goodman and Kieffer [17] and Jaeger [18] outlined several simple methods and their limitations for estimating strength and stability of rock slopes. Due to the advancement of various computational techniques, our ability to more accurately evaluate rock slope stability and interpret the likely failure mechanisms has improved [19]. Buhan et al. [20] found that the final results of a stability analysis may be influenced by scale effect of rock masses. Sonmez et al. [21] utilised back analysis of slope failures to obtain rock slope strength parameters. In their study, the applicability of rock mass classification, and a practical procedure of estimating the mobilised shear strength based on the Hoek–Brown yield criterion were explained. Previous investigations [22–25] of progressive failures and/or safety factor assessment of rock slopes have used a range of numerical methods. These include the continuum methods (finite element method and the finite difference method), the discontinuum methods (distinct element and discontinuous deformation analysis), and finite-/discrete-element codes. In addition, the probabilistic analytical method is employed in [26,27] to find the rock slope potential failure key-group and estimate the probability of failure. It should be acknowledged that the slope stability probability classification proposed by Hack et al. [27] does not require cohesion and friction as input. Yang et al. [28–30] adopted tangential strength parameters (c and ϕ) from the Hoek–Brown failure criterion in an upper bound analysis to obtain the optimised height of a slope. As far as the authors are aware, these studies [28–30] represent the only attempt at providing slope stability factors for estimating rock slope stability.

Currently, practising engineers typically use a number of stability charts when attempting to predict the stability of rock slopes: (1) Hoek–Bray [1] charts can be used for rock and rockfill slopes; (2) Zanbak [31] proposed a set of stability charts for rock slopes susceptible to toppling; (3) stability charts were presented by Siad [32] based on the upper bound approach that can be used for rock slopes with earthquake effects. However, these three sets of design charts require conventional Mohr–Coulomb soil parameters, cohesion (c) and friction angle (ϕ), as input. From a review of the literature, the authors are not aware of any slope stability chart solutions based on the native form of the Hoek–Brown failure criterion that requires Hoek–Brown material parameters as input. This paper is concerned with providing a set of stability charts for rock slopes based on the Hoek–Brown failure criterion that can be used by practising engineers to rapidly assess the preliminary stability of rock slopes.

3. The generalised Hoek–Brown failure criterion

3.1. Applicability

Practitioners are often required to predict the strength of large-scale rock masses for design. Fortunately, Hoek and Brown [6] proposed an empirical failure criterion which developed through curve fitting of triaxial test data suited for intact rock and jointed rock masses. The criterion is based on a classification system called the Geological Strength Index (*GSI*). The Hoek–Brown criterion is one of the few non-linear criteria widely accepted and used by engineers to estimate the strength of a rock mass. Therefore, it is appropriate to use this criterion when assessing the stability of istopic rock slopes in this study.

The *GSI* classification system is based upon the assumption that the rock mass contains sufficient number of "randomly" oriented discontinuities such that it behaves as an isotropic mass. In other words, the behaviour of the rock mass is independent of the direction of the applied loads. Therefore, it is clear that the *GSI* system should not be applied to those rock masses in which there is a clearly defined dominant structural orientation that will lead to highly anisotropic mechanical behaviour. In addition, it is also inappropriate to assign *GSI* values to excavated faces in strong hard rock with a few discontinuities spaced at distances of similar magnitude to the dimensions of slope under consideration. In such cases the stability of the slope will be controlled by the three-dimensional geometry of the intersecting discontinuities and the free faces created by the excavation.

In line with the above discussion, it is important to realise the stability charts presented in this paper will be subject to the same limitations that underpin the Hoek–Brown yield criterion itself. An excellent overview of the applicability and limitations of the *GSI* system can be found in [33].

An explanation for the applicability of Hoek–Brown criterion when applied to rock slopes is displayed in Fig. 1. After Hoek [34], for the same rock properties throughout the slope, rock masses can be classified into three structural groups, namely Group I, Group II and Group III. Fig. 1 shows the transition from an isotropic intact rock (Group I), through a highly anisotropic rock mass (Group II), to a heavily jointed rock mass (Group III). In this paper the rock slope has been assumed to be either (1) intact or; (2) heavily jointed so that, on the scale of the problem, it can be regarded as an isotropic assembly of interlocking particles. In the case of intact rock (Group I), it should be noted that the failure mechanism of intact rock may be brittle rather than plastic, so the theories of plasticity may not be appropriate.

3.2. Numerical implementation

The upper-bound and lower-bound methods developed in [12–14] can deal with a wide range of yield criteria; however, on deviatoric planes the surfaces of those criteria must be convex and smooth. The Hoek–Brown yield surface has apex and corner singularities in stress space, and therefore numerical smoothing is required to avoid singularities. Details of the implementation of the Hoek–Brown criterion into the numerical limit analysis formulations can be found in [16] and will not be repeated here. In this study, the latest version of Hoek–Brown failure criterion [11] is employed.

$$\sigma_1' = \sigma_3' + \sigma_{ci}\left(m_b\frac{\sigma_3'}{\sigma_{ci}} + s\right)^{\alpha}, \tag{1}$$

where

$$m_b = m_i \exp\left(\frac{GSI - 100}{28 - 14D}\right), \tag{2}$$

$$s = \exp\left(\frac{GSI - 100}{9 - 3D}\right), \tag{3}$$

$$\alpha = \frac{1}{2} + \frac{1}{6}\left(e^{-GSI/15} - e^{-20/3}\right). \tag{4}$$

The *GSI* was introduced because Bieniawski's rock mass rating (RMR) system [35] and the Q-system [36] were deemed to be unsuitable for poor rock masses. The *GSI* ranges from about 10, for extremely poor rock masses, to 100 for intact rock. The parameter D is a factor that depends on the degree of disturbance. The suggested value of disturbance factor is $D = 0$ for undisturbed in situ rock masses and $D = 1$ for disturbed rock mass properties. The magnitude of the disturbance factor is affected by blast damage and stress relief due to overburden removal. For the analyses presented here, a value of $D = 0$ has been adopted.

The uniaxial compressive strength is obtained by setting $\sigma_3 = 0$ in Eq. (1), giving

$$\sigma_c = \sigma_{ci} s^{\alpha}, \tag{5}$$

and the tensile strength is

$$\sigma_t = -\frac{s\sigma_{ci}}{m_b}. \tag{6}$$

3.3. Equivalent Mohr–Coulomb parameters

Since most geotechnical engineering software is still written in terms of the Mohr–Coulomb failure criterion, it is necessary for practising engineers to determine equivalent friction angles and cohesive strengths for each rock mass and stress range. In the context of this paper, the solutions obtained by using equivalent Mohr–Coulomb

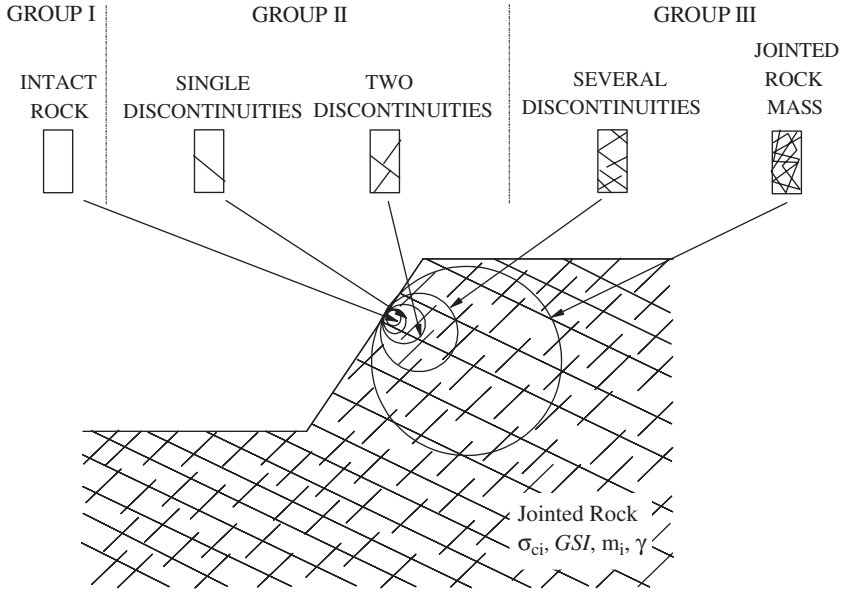

Fig. 1. Applicability of the Hoek–Brown failure criterion for slope stability problems.

parameters can be compared directly with the solutions from using the native Hoek–Brown failure criterion.

Fig. 2 is an illustration of the Hoek–Brown criterion and equivalent Mohr–Coulomb envelope. Because the equivalent Mohr–Coulomb envelope is a straight line, it cannot fit the Hoek–Brown curve completely. If we divide Fig. 2 into three zones, namely Region 1, Region 2, and Region 3, it can be seen that when rock stress conditions fall in Regions 1 and 3, using equivalent Mohr–Coulomb parameters may overestimate the ultimate shear strength when compared with the Hoek–Brown curve. Regarding the fitting process, more details can be found in Hoek et al. [11] where the process involves balancing the areas above and below the Mohr–Coulomb plot over a range of minor principal stress values. This results in the following equations for friction angle and cohesive strength

$$c' = \frac{\sigma_{ci}\left[(1+2\alpha)s + (1-\alpha)m_b\sigma'_{3n}\right](s+m_b\sigma'_{3n})^{\alpha-1}}{(1+\alpha)(2+\alpha)\sqrt{1+\left(6\alpha m_b(s+m_b\sigma'_{3n})^{\alpha-1}\right)/(1+\alpha)(2+\alpha)}}, \tag{7}$$

$$\phi' = \sin^{-1}\left[\frac{6\alpha m_b(s+m_b\sigma'_{3n})^{\alpha-1}}{2(1+\alpha)(2+\alpha)+6\alpha m_b(s+m_b\sigma'_{3n})^{\alpha-1}}\right] \tag{8}$$

where $\sigma_{3n} = \sigma'_{3max}/\sigma_{ci}$.

It should be noted that the value of σ'_{3max} has to be determined for each particular problem. For slope stability problems, Hoek et al. [11] suggests σ'_{3max} can be estimated by the following equation:

$$\frac{\sigma'_{3max}}{\sigma'_{cm}} = 0.72\left[\frac{\sigma'_{cm}}{\gamma H}\right]^{-0.91}, \tag{9}$$

in which H is the height of the slope and γ is the material unit weight. For the stress range, $\sigma_t < \sigma'_3 < \sigma_{ci}/4$, the compressive strength of the rock mass σ'_{cm} can be determined as

$$\sigma'_{cm} = \sigma_{ci}\frac{(m_b+4s-\alpha(m_b-8s))(m_b/4+s)^{\alpha-1}}{2(1+\alpha)(2+\alpha)}. \tag{10}$$

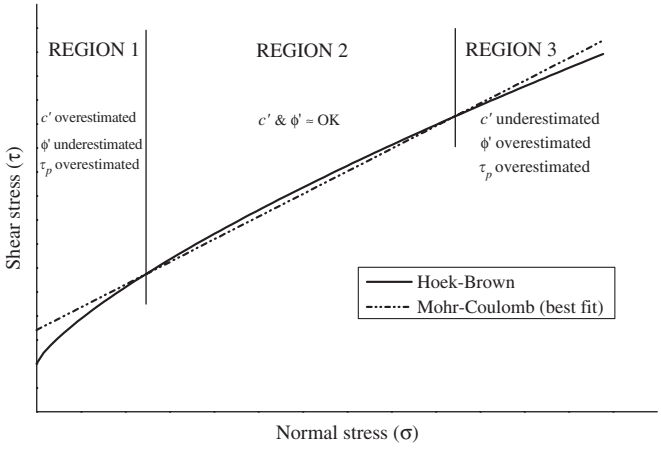

Fig. 2. Hoek–Brown and equivalent Mohr–Coulomb criteria.

4. Problem definition

A plane strain illustration of the slope-stability problem is shown in Fig. 3, where the jointed rock mass has an intact uniaxial compressive strength σ_{ci}, *GSI*, intact rock yield parameter m_i, and unit weight γ. The rock weight γ can be estimated from core samples and σ_{ci} and m_i can be obtained from either triaxial test results or from the tables proposed in [37]. Several approaches can be used to evaluate *GSI* as outlined in [37], which include using table solutions and estimating by using *RMR* [35]. Excavated slope and tunnel faces are probably the most reliable source of information for *GSI* estimates. Hoek and Brown [38] also pointed out that *GSI* can be adjusted to a smaller magnitude in order to incorporate the effects of surface weathering. Greater detail on how to best estimate the Hoek–Brown material parameters can be found in Hoek and Brown [38], Hoek [37] and Wyllie and Mah [3].

In this study, all the quantities are assumed constant throughout the slope. In the limit analyses, for given slope geometry (H,β) and rock mass (σ_{ci},*GSI*,m_i), the optimised solutions of the upper-bound and lower-bound programs can be carried out with respect to the unit weight, γ. In this study, slope inclinations of $\beta = 15^\circ$, 30°, 45°, 60°, and 75° are analysed. The effect of depth factor (d/H) was found to be insignificant. With the exception of the case where $\beta = 15^\circ$, all analyses indicated the primary failure mode was one where the slip line passed through the toe of the slope (toe failure). The dimensionless stability number is defined as

$$N = \frac{\sigma_{ci}}{\gamma H F}, \tag{11}$$

where F is the safety factor of the slope.

5. Results and discussion of limit analyses

5.1. Limit analysis solutions

Figs. 4–8 present stability charts from the numerical upper- and lower-bound formulations for angles of $\beta = 15^\circ$–75° for a range of *GSI* and m_i. The stability number N was defined in Eq. (11). Referring to Fig. 4, it is apparent that the upper- and lower-bound results bracket a narrow range of stability numbers N for $GSI = 10$, so an

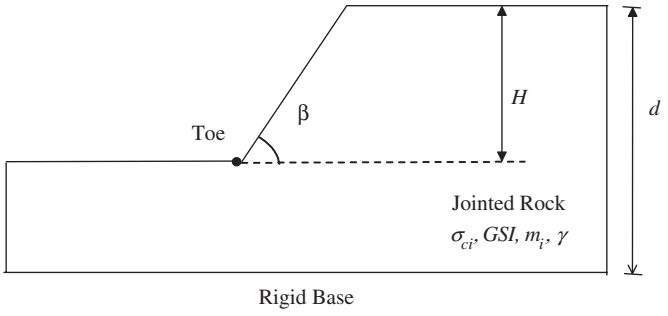

Fig. 3. Problem definition.

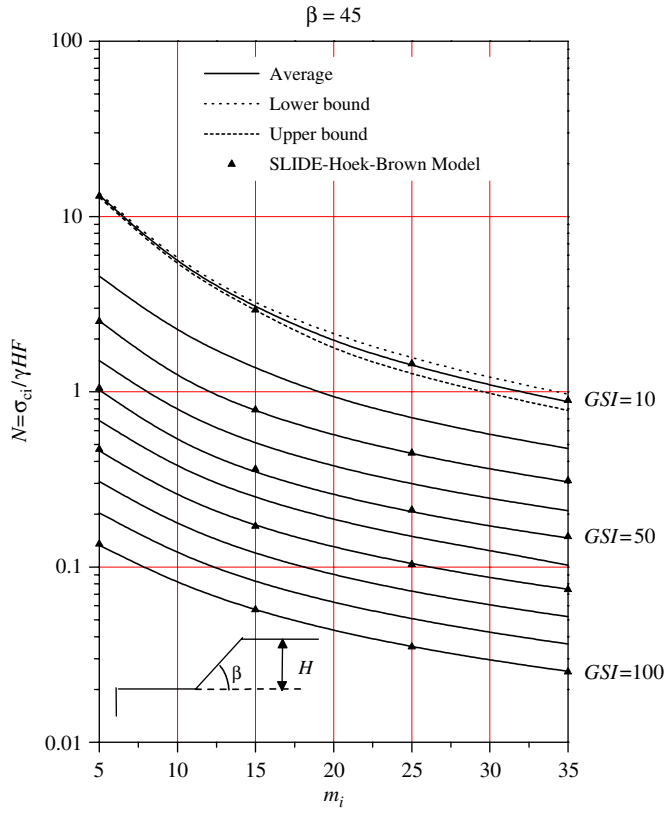

Fig. 4. Average finite element limit analysis solutions of stability numbers ($\beta = 45°$).

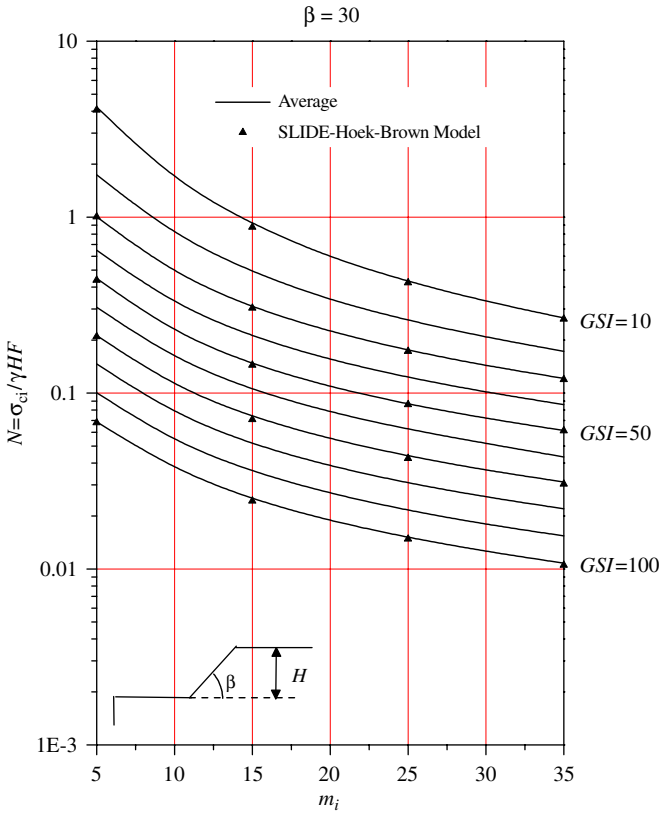

Fig. 6. Average finite element limit analysis solutions of stability numbers ($\beta = 30°$).

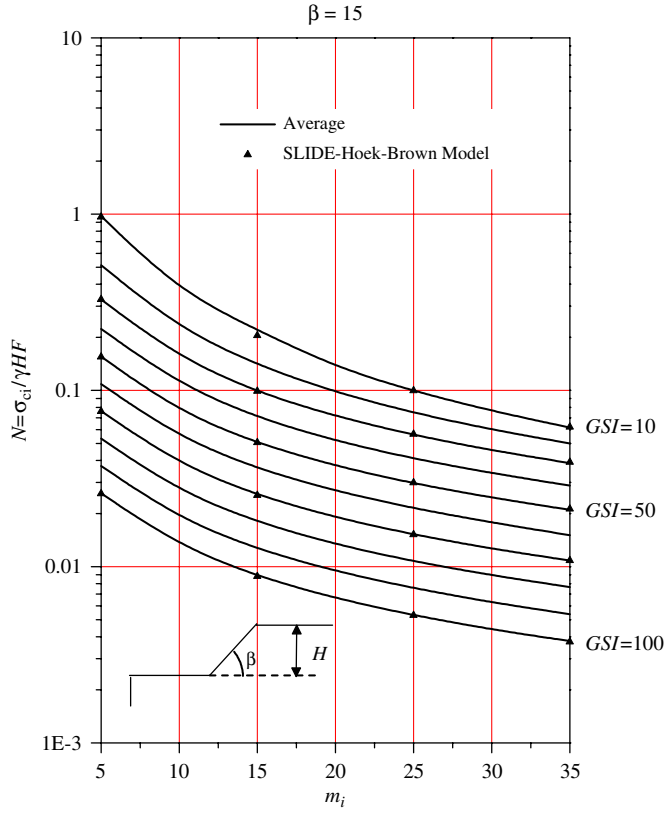

Fig. 5. Average finite element limit analysis solutions of stability numbers ($\beta = 15°$).

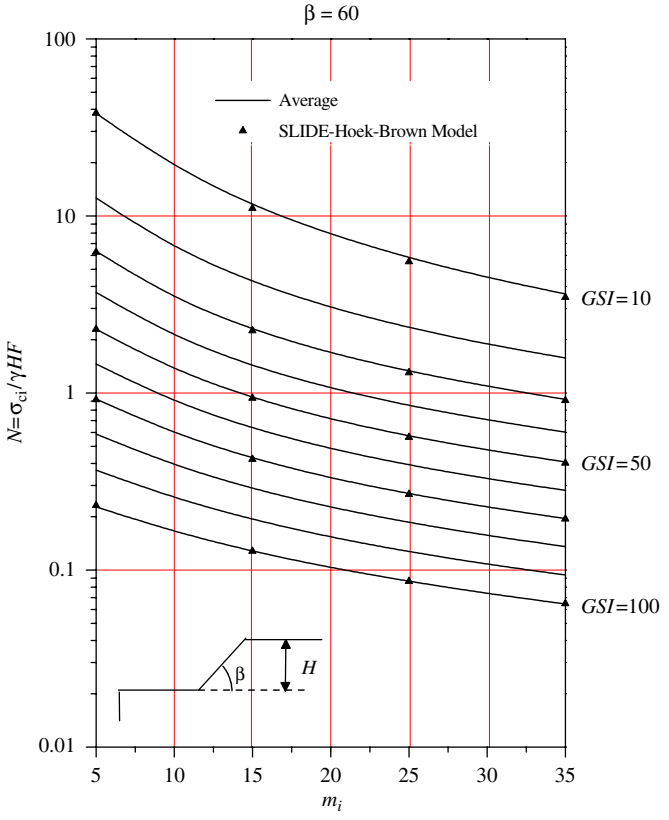

Fig. 7. Average finite element limit analysis solutions of stability numbers ($\beta = 60°$).

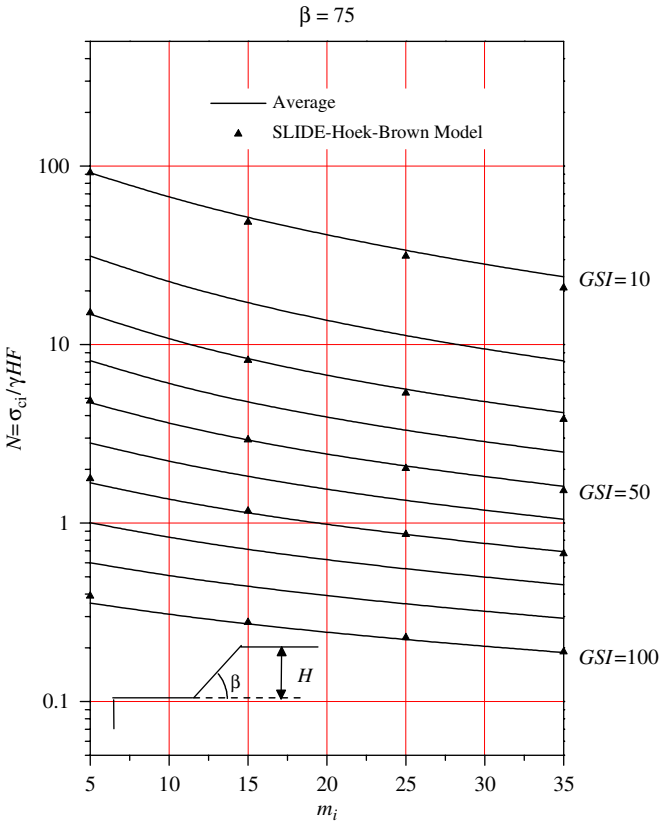

Fig. 8. Average finite element limit analysis solutions of stability numbers ($\beta = 75°$).

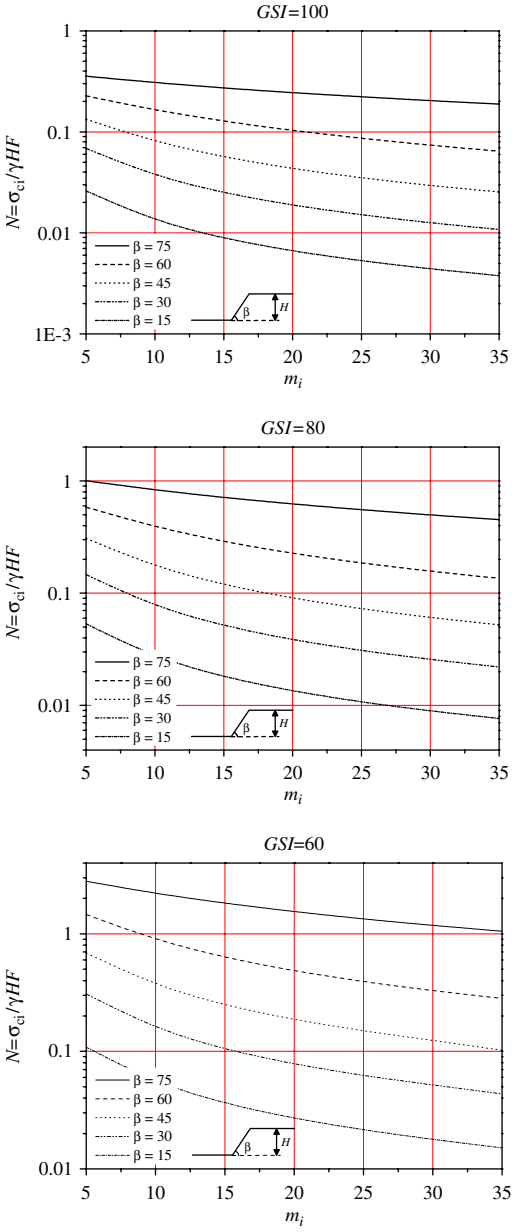

Fig. 9. Average finite element limit analysis solutions of stability numbers ($GSI = 100$, 80 and 60).

average value from the bound solutions could be adopted for simplicity. In fact, it was found that, for all the analyses performed, the range between upper- and lower-bound stability numbers was always less than $\pm 5\%$. The only exception to this observation occurs for the cases of $\beta = 45°$ and low *GSI* values, where the range is around $\pm 9\%$. Therefore, average values of the stability number N have been adopted and presented unless stated otherwise. The parameter N can be seen to decrease as the value of *GSI* or m_i increases.

Figs. 9 and 10 show an alternative form of stability charts as a function of the slope angle, β. The users only need to estimate *GSI* and m_i for the rock mass, and then the stability number can be estimated for a given slope angle. For the same rock slope material, the differences in stability number between various slope angles can provide a ratio of safety factor. For example, it can be found that decreasing slope angles from $\beta = 75°$ to 60° for $GSI = 80$ can increase the factor of safety by more than 50%.

Referring to the above results, for any given rock mass (σ_{ci}, *GSI*, m_i) and unit weight of the material γ, the obtained stability number can be used to determine the ultimate height of cut slopes. In addition, the charts indicate that the stability number N increases with increasing slope angle for a given *GSI* and m_i.

Fig. 11 displays several of the observed upper-bound plastic zones for different slope angles in which $H = 1$. The depth of failure surface increases with the reduction in the slope angle. But this variation cannot be found when the slope angle $\beta > 45°$. For a given *GSI*, it was found that the depth of plastic zone is almost unchanged with increasing m_i.

5.2. Application example

The stability charts illustrated in Figs. 4–8 provide an efficient method to determine the factor of safety F for a rock slope. The following example is of a slope constructed in a very poor quality rock mass. It has the following parameters: the slope angle $\beta = 60°$, the height of the slope $H = 25$ m, the intact uniaxial compressive strength

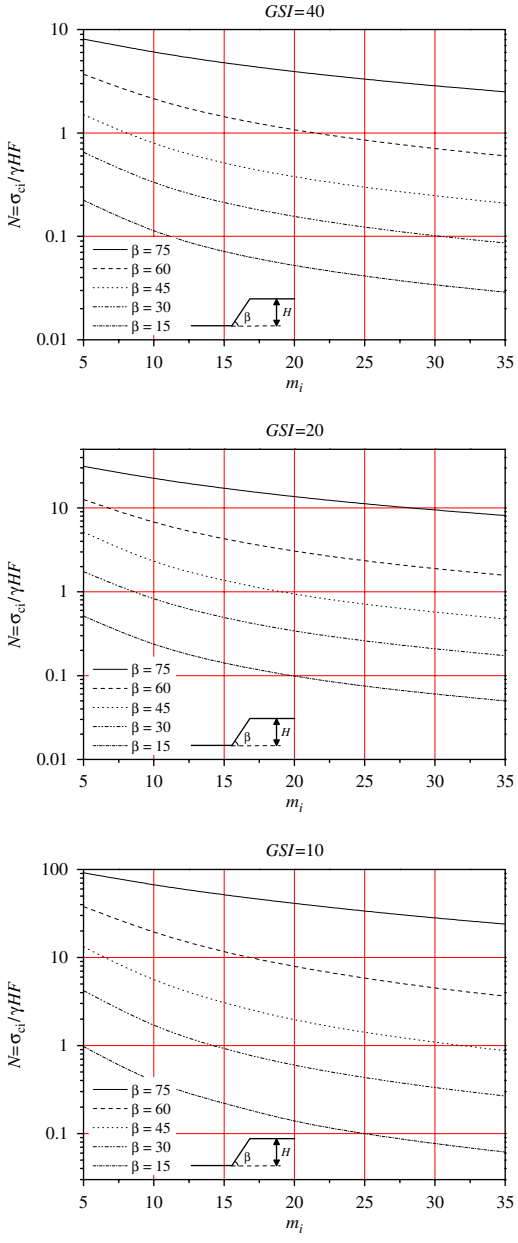

Fig. 10. Average finite element limit analysis solutions of stability numbers $GSI = 40$, 20 and 10).

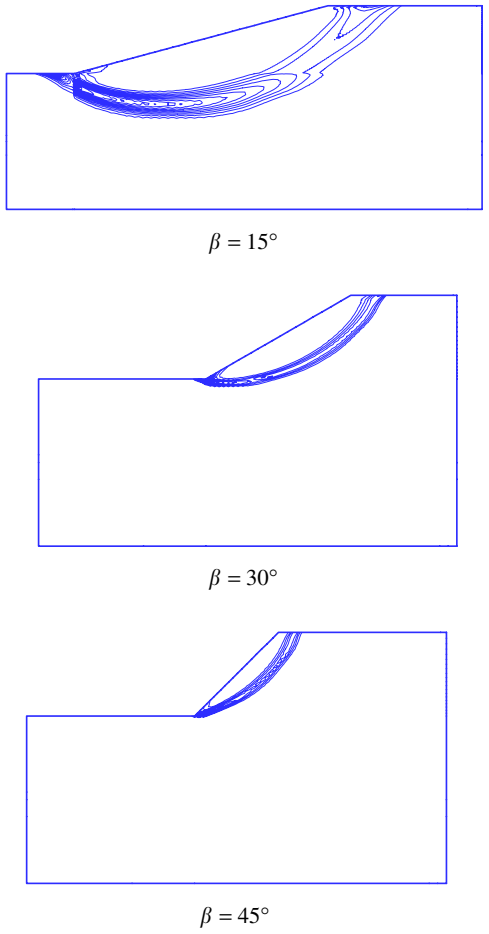

Fig. 11. Upper bound plastic zones with the different slope angles ($GSI = 70$ and $m_i = 15$).

$\sigma_{ci} = 20$ MPa, $GSI = 30$, intact rock yield parameter $m_i = 8$, and unit weight of rock mass $\gamma = 23\,\mathrm{kN/m^3}$. With this information, the safety factor (F) of this rock slope can be obtained as follows. First, from the values of σ_{ci}, γ and H, we can calculate a dimensionless parameter $\sigma_{ci}/\gamma H = 20000/(23 \times 25) = 34.8$. In Fig. 7, $N = \sigma_{ci}/\gamma HF \approx 4$. The factor of safety can then be calculated as $F = 34.8/4 = 8.7$.

6. Results and discussion of limit equilibrium analyses

In general, rock slope stability is more often analysed using the limit equilibrium method and equivalent Mohr–Coulomb parameters as determined by Eqs. (7) and (8). With this being the case, an obvious question is how do the limit equilibrium results using equivalent Mohr–Coulomb parameters compare with the limit analysis results using the Hoek–Brown criterion. In order to make this comparison, the commercial limit equilibrium software SLIDE [39] and Bishop's simplified method [40] have been used. The software SLIDE can perform a slope analysis using the Mohr–Coulomb yield or the generalised Hoek–Brown criterion. When the Mohr–Coulomb criterion is used, the cohesion (c) and friction angle (ϕ) are constant along any given slip surface and are independent of the normal stress as expected. However, when the Hoek–Brown criterion is selected, the software will calculate a set of instantaneous equivalent Mohr–Coulomb parameters when analysing the slope based on the normal stress at the base of each individual slice. More details on how the parameters are actually calculated can be found in [37]. Therefore, the cohesion (c) and the friction angle (ϕ) will vary along any given slip surface. By calculating equivalent Mohr–Coulomb parameters in this way, a more accurate representation of the curved nature of the Hoek–Brown criterion in τ–σ_n space is obtained. Referring to Figs. 4–8, the triangular points shown represent the stability numbers obtained from the limit equilibrium method based on the

Hoek–Brown strength parameters. It can be found that these points are remarkably close to the average lines of the limit analysis solutions and most of them locate between the upper and lower bound solutions.

For the given materials and geometrical properties of the slope, the finite element lower bound analysis will provide the optimum unit weight (γ) such that collapse has just occurred (i.e., $F=1$). A critical non-dimensional parameter $(\sigma_{ci}/\gamma H)_{crit}$ can then be defined for the subsequent SLIDE analyses. In Table 1, the safety factor ($F1$) and ($F2$) are obtained using the Hoek–Brown criterion and the Mohr–Coulomb criterion in SLIDE, respectively. Both these analyses are based on equivalent Mohr–Coulomb parameters with the only difference being how these parameters are calculated (as discussed above).

The comparisons of the safety factors F, $F1$ and $F2$ are shown in Table 1 where the largest difference between F and $F1$ and F and $F2$ are about 4 and 64%, respectively. This shows that the results of SLIDE analyses using the Hoek–Brown model compare well with the results of the lower-bound limit analyses. In contrast the results of SLIDE analyses using the Mohr–Coulomb model do not compare favourably with the lower-bound results. From Table 1, it can be found that using the Mohr–Coulomb model may lead to significant overestimations of safety factors, particularly for steep slopes. The average difference between F and $F2$ for $\beta=60^\circ$ and 75° was found to be 16.8% and 34.3%, respectively. For all cases, the average overestimation is 12.8%. It should be stressed that, a high estimation of safety factor will induce a non-conservative design. It was found that using the Hoek–Brown model in SLIDE will produce a failure mechanism in good agreement with the upper-bound mechanism. The same could not be said when using the Mohr–Coulomb model. For $\beta=30^\circ$, both of the above models achieve similar failure surfaces, which agree well with the upper-bound plastic zone. In almost all cases, a toe-failure mode was observed, the only exception being the case of $\beta=15^\circ$ (base failure).

In order to determine the source of overestimations in factors of safety ($F2$) for steep slopes, the stress conditions

Table 1
Comparisons of safety factors between the Hoek–Brown strength parameters and the equivalent Mohr–Coulomb parameters

			Limit analysis-lower bound		SLIDE-limit equilibrium using equivalent Mohr–Coulomb parameters							
			Nonlinear Hoek–Brown		Nonlinear Hoek–Brown		Eqs. (7), (8) and (9) Linear Mohr–Coulomb		Eqs. (7), (8) and (12) Linear Mohr–Coulomb		Eqs. (7), (8) and (13) Linear Mohr–Coulomb	
β	GSI	m_i	$(\sigma_{ci}/\gamma H)_{crit}$	F	$F1$	%Diff	$F2$	%Diff	$F3$	%Diff	$F4$	%Diff
75	100	5	0.360	1	0.963	−3.7%	1.008	1%	1.028	3%	–	–
75	100	15	0.278	1	0.999	−0.1%	1.164	16%	1.042	4%	–	–
75	100	25	0.228	1	1.002	0.2%	1.218	22%	1.079	8%	–	–
75	100	35	0.194	1	1.004	0.4%	1.286	29%	1.112	11%	–	–
75	70	5	1.703	1	0.988	−1.2%	1.081	8%	1.025	2%	–	–
75	70	15	1.169	1	1.002	0.2%	1.287	29%	1.081	8%	–	–
75	70	25	0.890	1	1.005	0.5%	1.35	35%	1.124	12%	–	–
75	70	35	0.717	1	1.016	1.6%	1.394	39%	1.156	16%	–	–
75	50	5	4.980	1	0.997	−0.3%	1.154	15%	1.036	4%	–	–
75	50	15	2.988	1	1.004	0.4%	1.336	34%	1.119	12%	–	–
75	50	25	2.156	1	1.018	1.8%	1.425	43%	1.148	15%	–	–
75	50	35	1.668	1	1.024	2.4%	1.45	45%	1.174	17%	–	–
75	30	5	15.011	1	1.001	0.1%	1.248	25%	1.047	5%	–	–
75	30	15	8.576	1	1.016	1.6%	1.459	46%	1.136	14%	–	–
75	30	25	5.824	1	1.025	2.5%	1.51	51%	1.173	17%	–	–
75	30	35	4.327	1	1.033	3.3%	1.516	52%	1.194	19%	–	–
75	10	5	93.721	1	1.004	0.4%	1.224	22%	1.018	2%	–	–
75	10	15	53.362	1	1.023	2.3%	1.504	50%	1.126	13%	–	–
75	10	25	35.186	1	1.035	3.5%	1.605	61%	1.185	19%	–	–
75	10	35	24.994	1	1.046	4.6%	1.642	64%	1.21	21%	–	–
60	100	5	0.232	1	1.001	0.1%	1.033	3%	1.043	4%	–	–
60	100	15	0.130	1	1.004	0.4%	1.114	11%	1.026	3%	–	–
60	100	25	0.088	1	1.004	0.4%	1.146	15%	1.035	3%	–	–
60	100	35	0.066	1	1.004	0.4%	1.141	14%	1.04	4%	–	–
60	70	5	0.946	1	1.013	1.3%	1.059	6%	1.024	2%	–	–
60	70	15	0.435	1	1.004	0.4%	1.143	14%	1.033	3%	–	–
60	70	25	0.276	1	1.004	0.4%	1.161	16%	1.043	4%	–	–
60	70	35	0.200	1	1.005	0.5%	1.183	18%	1.047	5%	–	–
60	50	5	2.337	1	1.005	0.5%	1.124	12%	1.026	3%	–	–
60	50	15	0.953	1	1.004	0.4%	1.171	17%	1.036	4%	–	–

Table 1 (*continued*)

			Limit analysis-lower bound		SLIDE-limit equilibrium using equivalent Mohr–Coulomb parameters							
			Nonlinear Hoek–Brown		Nonlinear Hoek–Brown		Eqs. (7), (8) and (9) Linear Mohr–Coulomb		Eqs. (7), (8) and (12) Linear Mohr–Coulomb		Eqs. (7), (8) and (13) Linear Mohr–Coulomb	
β	*GSI*	m_i	$(\sigma_{ci}/\gamma H)_{crit}$	*F*	*F*1	%Diff	*F*2	%Diff	*F*3	%Diff	*F*4	%Diff
60	50	25	0.584	1	1.008	0.8%	1.176	18%	1.046	5%	–	–
60	50	35	0.419	1	1.009	0.9%	1.172	17%	1.049	5%	–	–
60	30	5	6.439	1	1.009	0.9%	1.15	15%	1.023	2%	–	–
60	30	15	2.317	1	1.009	0.9%	1.197	20%	1.044	4%	–	–
60	30	25	1.356	1	1.01	1.0%	1.201	20%	1.049	5%	–	–
60	30	35	0.945	1	1.011	1.1%	1.23	23%	1.051	5%	–	–
60	10	5	38.926	1	1.004	0.4%	1.183	18%	1.013	1%	–	–
60	10	15	11.734	1	1.013	1.3%	1.257	26%	1.048	5%	–	–
60	10	25	5.928	1	1.017	1.7%	1.261	26%	1.054	5%	–	–
60	10	35	3.729	1	1.018	1.8%	1.258	26%	1.059	6%	–	–
45	100	5	0.135	1	1	0.0%	1.008	1%	1.022	2%	1.027	3%
45	100	15	0.058	1	1.005	0.5%	1.041	4%	1.003	0%	1.086	9%
45	100	25	0.036	1	1.012	1.2%	1.047	5%	1.003	0%	1.11	11%
45	100	35	0.026	1	1.015	1.5%	1.06	6%	1.005	0%	1.126	13%
45	70	5	0.469	1	1.001	0.1%	1.038	4%	1.001	0%	1.055	5%
45	70	15	0.176	1	1.012	1.2%	1.08	8%	1.002	0%	1.098	10%
45	70	25	0.108	1	1.017	1.7%	1.06	6%	1.007	1%	1.113	11%
45	70	35	0.077	1	1.019	1.9%	1.061	6%	1.009	1%	1.123	12%
45	50	5	1.046	1	1.004	0.4%	1.045	4%	1.001	0%	1.063	6%
45	50	15	0.369	1	1.009	0.9%	1.065	6%	1.004	0%	1.098	10%
45	50	25	0.222	1	1.02	2.0%	1.066	7%	1.01	1%	1.11	11%
45	50	35	0.158	1	1.021	2.1%	1.044	4%	1.011	1%	1.118	12%
45	30	5	2.593	1	1.011	1.1%	1.066	7%	0.999	0%	1.06	6%
45	30	15	0.829	1	1.018	1.8%	1.07	7%	1.007	1%	1.094	9%
45	30	25	0.480	1	1.021	2.1%	1.076	8%	1.01	1%	1.11	11%
45	30	35	0.334	1	1.024	2.4%	1.085	9%	1.011	1%	1.118	12%
45	10	5	13.585	1	1.014	1.4%	1.087	9%	1	0%	1.039	4%
45	10	15	3.155	1	1.023	2.3%	1.106	11%	1.005	0%	1.08	8%
45	10	25	1.552	1	1.023	2.3%	1.107	11%	1.009	1%	1.103	10%
45	10	35	0.969	1	1.026	2.6%	1.079	8%	1.01	1%	1.115	12%
30	100	5	0.070	1	1.014	1.4%	0.988	−1%	–	–	1	0%
30	100	15	0.026	1	1.02	2.0%	0.999	0%	–	–	1.024	2%
30	100	25	0.016	1	1.023	2.3%	1.003	0%	–	–	1.036	4%
30	100	35	0.011	1	1.024	2.4%	1.007	1%	–	–	1.044	4%
30	70	5	0.218	1	1.018	1.8%	0.985	−2%	–	–	1.011	1%
30	70	15	0.075	1	1.023	2.3%	0.996	0%	–	–	1.028	3%
30	70	25	0.045	1	1.024	2.4%	1.004	0%	–	–	1.035	3%
30	70	35	0.032	1	1.025	2.5%	1.01	1%	–	–	1.04	4%
30	50	5	0.461	1	1.02	2.0%	0.993	−1%	–	–	1.014	1%
30	50	15	0.153	1	1.024	2.4%	1.003	0%	–	–	1.026	3%
30	50	25	0.091	1	1.025	2.5%	1.024	2%	–	–	1.032	3%
30	50	35	0.065	1	1.026	2.6%	1.008	1%	–	–	1.036	4%
30	30	5	1.057	1	1.022	2.2%	1.001	0%	–	–	1.012	1%
30	30	15	0.323	1	1.026	2.6%	1.003	0%	–	–	1.026	3%
30	30	25	0.185	1	1.026	2.6%	1.005	0%	–	–	1.031	3%
30	30	35	0.129	1	1.027	2.7%	1.004	0%	–	–	1.035	3%
30	10	5	4.363	1	1.023	2.3%	1.002	0%	–	–	1.006	1%
30	10	15	0.943	1	1.025	2.5%	1.007	1%	–	–	1.023	2%
30	10	25	0.460	1	1.026	2.6%	0.996	0%	–	–	1.033	3%
30	10	35	0.286	1	1.026	2.6%	1.004	0%	–	–	1.04	4%
10	100	5	0.026	1	1.009	0.9%	1.067	7%	–	–	1	0%
10	100	15	0.009	1	1.011	1.1%	1.079	8%	–	–	0.987	−1%
10	100	25	0.005	1	1.011	1.1%	1.091	9%	–	–	0.985	−2%
10	100	35	0.004	1	1.012	1.2%	1.094	9%	–	–	0.986	−1%
10	70	5	0.078	1	1.01	1.0%	1.069	7%	–	–	0.994	−1%
10	70	15	0.026	1	1.01	1.0%	1.087	9%	–	–	0.987	−1%

Table 1 (*continued*)

			Limit analysis-lower bound		SLIDE-limit equilibrium using equivalent Mohr–Coulomb parameters							
			Nonlinear Hoek–Brown		Nonlinear Hoek–Brown		Eqs. (7), (8) and (9) Linear Mohr–Coulomb		Eqs. (7), (8) and (12) Linear Mohr–Coulomb		Eqs. (7), (8) and (13) Linear Mohr–Coulomb	
β	*GSI*	m_i	$(\sigma_{ci}/\gamma H)_{crit}$	*F*	*F*1	%Diff	*F*2	%Diff	*F*3	%Diff	*F*4	%Diff
10	70	25	0.015	1	1.011	1.1%	1.091	9%	–	–	0.985	−2%
10	70	35	0.011	1	1.011	1.1%	1.094	9%	–	–	0.985	−2%
10	50	5	0.158	1	1.01	1.0%	1.067	7%	–	–	0.996	0%
10	50	15	0.052	1	1.01	1.0%	1.055	5%	–	–	0.989	−1%
10	50	25	0.031	1	1.011	1.1%	1.081	8%	–	–	0.986	−1%
10	50	35	0.022	1	1.011	1.1%	1.084	8%	–	–	0.985	−2%
10	30	5	0.334	1	1.01	1.0%	1.05	5%	–	–	0.997	0%
10	30	15	0.101	1	1.011	1.1%	1.068	7%	–	–	0.99	−1%
10	30	25	0.058	1	1.011	1.1%	1.072	7%	–	–	0.988	−1%
10	30	35	0.040	1	1.011	1.1%	1.075	8%	–	–	0.986	−1%
10	10	5	0.994	1	1.012	1.2%	1.036	4%	–	–	0.994	−1%
10	10	15	0.211	1	1.013	1.3%	1.039	4%	–	–	0.985	−2%
10	10	25	0.103	1	1.013	1.3%	1.041	4%	–	–	0.985	−2%
10	10	35	0.064	1	1.013	1.3%	1.032	3%	–	–	0.986	−1%

on each slice from the SLIDE limit equilibrium analyses were observed more closely. It was found that, for steep slopes, the stress conditions of the slices along the failure plane tend to be located in Region 1 (Fig. 2) where the shape of the Hoek–Brown and Mohr–Coulomb strength criterions differs the greatest. In this region, at the same normal stress, the ultimate shear strength using the Hoek–Brown criterion is smaller than that of the Mohr–Coulomb criterion. Therefore, it is reasonable to conclude that using the equivalent Mohr–Coulomb parameters will provide a higher estimate of the safety factor.

From the results of this study, it appears that the equivalent parameters (c and ϕ) obtained from Eqs. (7–10) will lead to an unconservative factor of safety estimate, particularly for steep slopes where $\beta \geqslant 45^\circ$. In order to improve the estimate of *F*2, it becomes apparent a better estimate of σ'_{3max}, and therefore a different form for Eq. (9), is required.

To determine a more appropriate value of σ'_{3max} to be used in Eqs. (7) and (8), a similar study as performed in [11] is conducted. In these studies, Bishop's simplified method and SLIDE is used to analyse the cases in Table 1. For a factor of safety of 1, the relationship between $\sigma'_{cm}/\gamma H$ and $\sigma'_{3max}/\sigma'_{cm}$ is illustrated in Figs. 12 and 13. The authors have tried to fit only one equation incorporating all data to replace Eq. (9), but this did not prove possible. Instead separate equations are presented for what is defined as steep slopes $\beta \geqslant 45^\circ$ and gentle slopes $\beta < 45^\circ$ as Eqs. (12) and (13), respectively:

$$\frac{\sigma'_{3max}}{\sigma'_{cm}} = 0.2\left[\frac{\sigma'_{cm}}{\gamma H}\right]^{-1.07} \quad \text{(steep slope } \beta \geqslant 45^\circ\text{)}, \tag{12}$$

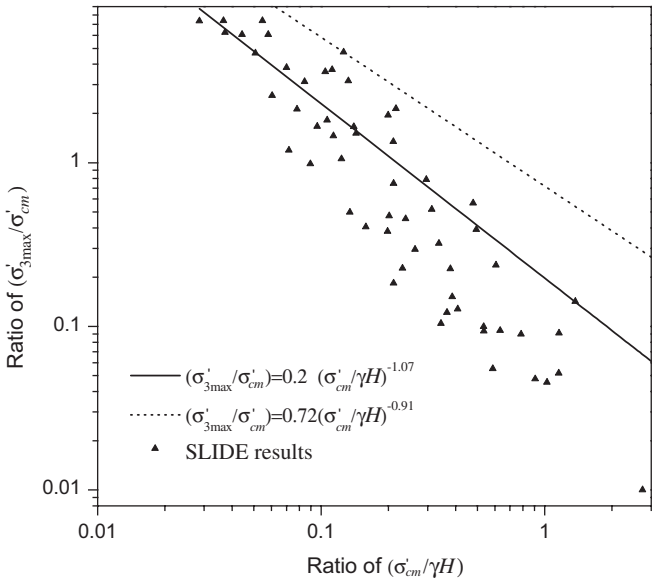

Fig. 12. Relationship for the calculation of σ'_{3max} between equivalent Mohr–Coulomb and Hoek–Brown parameters for steep slopes ($\beta \geqslant 45^\circ$).

$$\frac{\sigma'_{3max}}{\sigma'_{cm}} = 0.41\left[\frac{\sigma'_{cm}}{\gamma H}\right]^{-1.23} \quad \text{(gentle slope } \beta < 45^\circ\text{)}. \tag{13}$$

It can be seen in Figs. 12 and 13 the newly fitted Eq. (12) for steep slopes plots below the original Equation (9) and the newly proposed Eq. (13) for gentle slopes plots above the original Equation (9). For this reason, it is apparent that one curve fit is not possible for all slope angles.

In Table 1, the safety factors *F*3 and *F*4 are obtained from SLIDE using Mohr–Coulomb parameters which are calculated by estimating σ'_{3max} from Equations. (12) and (13). Comparing *F*3 and *F*4 with *F*2, shows that for steep

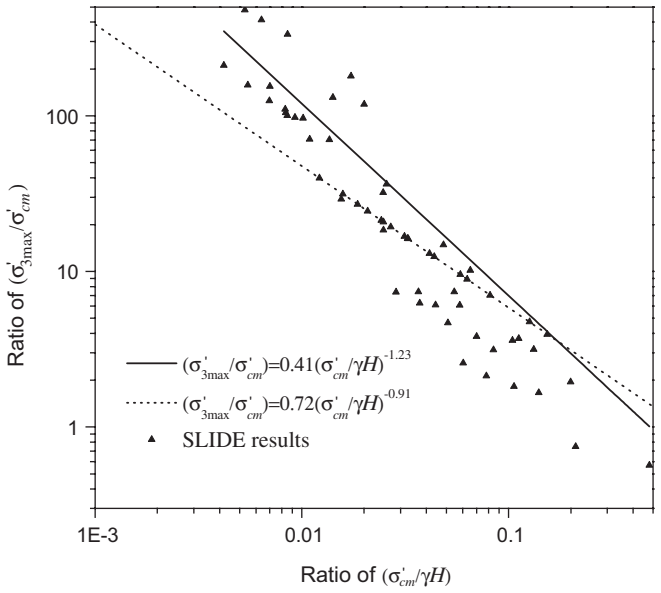

Fig. 13. Relationship for the calculation of σ'_{3max} between equivalent Mohr–Coulomb and Hoek–Brown parameters for gentle slopes ($\beta<45^\circ$).

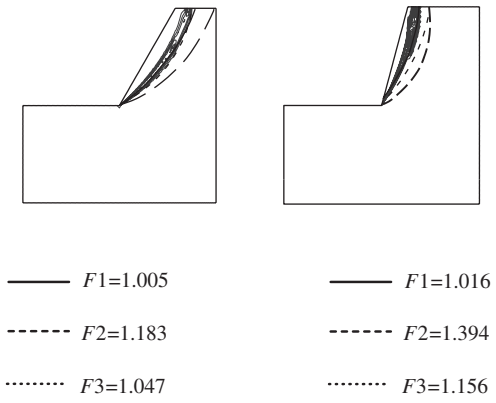

Fig. 14. Comparison between upper-bound plastic zones and failure surfaces from different strength parameters ($GSI = 70$ and $m_i = 35$).

slope, the safety factors estimates are much improved. A summary of the results in Table 1 shows that, using newly proposed equations to calculate the equivalent Mohr–Coulomb parameters, the largest difference of safety factor has decreased from 64% to 21% and the average difference has reduced from 12.8% to 3.4%. Thus, it can be concluded that using the modified Eqs. (12) and (13) will provide better results of safety factors which are, on average, only 3.4% higher than the lower-bound results. The newly proposed Eqs. (12) and (13) are both applicable in estimating σ'_{3max} for $\beta = 45^\circ$ cases. The results show that the difference in safety factor between these two equations is less than 8%. This would be acceptable for preliminary assessment of rock slope stability.

Fig. 14 displays the upper-bound plastic zones compared with failure surfaces obtained using SLIDE and different strength parameters from Eqs. (12) and (13). $F1$, $F2$, and $F3$ denote the safety factors obtained from using the Hoek–Brown (σ_{ci}, GSI, m_i, D), the original equivalent Mohr–Coulomb (proposed by Hoek), and the new equivalent Mohr–Coulomb (proposed in this paper) strength parameters, respectively. It is shown that using the original estimated Mohr–Coulomb parameters in analyses gives poor assessment of the stability and predictions of failure surfaces for steep slopes. On the other hand, by using the newly proposed equivalent Mohr–Coulomb parameters the predicted failure mechanism compares more favourably with the upper-bound mechanism and the factor of safety is much improved.

7. Conclusions

Stability charts based on the Hoek–Brown failure criterion are presented using formulations of the upper- and lower-bound limit theorems. These chart solutions can be used for estimating rock slope stability for preliminary design. It is important that users understand the assumptions and limitations before using these new rock slope stability charts. In particular, it should be noted that the chart solutions proposed in this paper are applicable to isotropic rock or rock masses only. Regarding the results of this study, the following conclusions can be made:

The upper-bound and lower-bound solutions bracket a narrow range of stability numbers (N) within $\pm 9\%$ or better (i.e. $\pm 5\%$) for all cases. This provides confidence that the true stability number has been bracketed accurately.

The general mode of failure for rock slopes was observed to be of the toe-failure type, except for the case of $\beta = 15^\circ$, where a base-failure type was observed.

The accuracy of using equivalent Mohr–Coulomb parameters for the rock mass in a traditional limit equilibrium method of slice analysis has been investigated. It was found that the factor of safety can be overestimated by up to 64% for steep slopes if existing guidelines for equivalent parameter determination are used. In order to improve the factor of safety estimate, 2 modified equations for steep and gentle slopes have been proposed. These equations are modifications of those originally proposed by Hoek [11]. When they are used to determine equivalent Mohr–Coulomb parameters that are subsequently used in a method of slice analysis, the factor of safety estimate is much improved and is at most 21% above the limit analysis result.

It was found that a limit equilibrium method of slice analysis can be used in conjunction with equivalent Mohr–Coulomb parameters to produce factor of safety estimates close to the limit analysis results, provided modifications are made to the underlying formulations. Such modifications have been made in the software SLIDE, where a set of equivalent Mohr–Coulomb parameters are calculated at the base of each individual slice. This approach predicts factors of safety remarkably close

to the limit analysis solutions that are based on the native form of the Hoek–Brown criterion.

References

[1] Hoek E, Bray JW. Rock slope engineering. 3rd ed. London: Institute of Mining and Metallurgy; 1981.

[2] Goodman RE. Introduction to rock mechanics. 2nd ed. New York: Wiley; 1989.

[3] Wyllie DC, Mah CW. Rock slope engineering. 4th ed. London: Spon Press; 2004.

[4] Taylor DW. Stability of earth slopes. J. Boston Soc Civ Eng 1937;24: 197–246.

[5] Gens A, Hutchinson JN, Cavounidis S. Three-dimensional analysis of slides in cohesive soils. Geotechnique 1988;38(1):1–23.

[6] Hoek E, Brown ET. Empirical strength criterion for rock masses. J Geotech Eng Div ASCE 1980;106(9):1013–35.

[7] Yu MH, Zan YW, Zhao J, Yoshimine M. A unified strength criterion for rock material. Int J Rock Mech Min Sci 2002;39:975–89.

[8] Grasselli G, Egger P. Constitutive law for the shear strength of rock joints based on three-dimensional surface parameters. Int J Rock Mech Min Sci 2003;40:25–40.

[9] Sheorey PR. Empirical rock failure criteria. Rotterdam: Balkema; 1997.

[10] Yudhbir, Lemanza W, Prinzl F. An empirical failure criterion for rock masses. In: Proceedings of the fifth Congress ISRM, 1983.

[11] Hoek E, Carranza-Torres C, Corkum B. Hoek-Brown Failure criterion-2002 edition. In: Proceedings of the North American Rock Mechanics Symposium Toronto, 2002.

[12] Lyamin AV, Sloan SW. Upper bound limit analysis using linear finite elements and non-linear programming. Int J Numer Anal Meth Geomech 2002;26:181–216.

[13] Lyamin AV, Sloan SW. Lower bound limit analysis using non-linear programming. Int J Numer Meth Eng 2002;55:573–611.

[14] Krabbenhoft K, Lyamin AV, Hjiaj M, Sloan SW. A new discontinuous upper bound limit analysis formulation. Int J Numer Meth Eng 2005;63:1069–88.

[15] Sutcliffe DJ, Yu HS, Sloan SW. Lower bound solutions for bearing capacity of jointed rock. Comput Geotech 2004;31:23–36.

[16] Merifield RS, Lyamin AV, Sloan SW. Limit analysis solutions for the bearing capacity of rock masses using the generalised Hoek-Brown criterion. Int J Rock Mech Min Sci 2006;43:920–37.

[17] Goodman RE, Kieffer DS. Behavior of rock in slope. J Geotech Geoenviron Eng 2000;126(8):675–84.

[18] Jaeger JC. Friction of rocks and stability of rock slopes. Geotechnique 1971;21(2):97–134.

[19] Stead D, Coggan JS, Eberhardt E. Realistic simulation of rock slope failure mechanisms: the need to incoporate principles of failure mechanisms. Int J Rock Mech Min Sci 2004;41(32B):17–22.

[20] Buhan PD, Freard J, Garnier D, Maghous S. Failure properties of fractured rock masses as anisotropic homogenized media. J Eng Mech 2002;128(8):869–75.

[21] Sonmez H, Ulusay R, Gokceoglu C. A practical procedure for the back analysis of slope failures in closely jointed rock masses. Int J Rock Mech Min Sci 1998;35(2):219–33.

[22] Hoek E, Read J, Karzulovic A, Chen ZY. Rock slopes in civil and mining engineering. In: Proceedings of the International Conference on Geotech Geol Eng, 2000, Melbourne.

[23] Wang C, Tannant DD, Lilly PA. Numerical analysis of stability of heavily jointed rock slopes using PFC2D. Int J Rock Mech Min Sci 2003;40:415–24.

[24] Eberhardt E, Stead D, Coggan JS. Numerical analysis of initiation and progressive failure in natural rock slopes—the 1991 Randa rockslide. Int J Rock Mech Min Sci 2004;41:69–87.

[25] Stead D, Eberhardt E, Coggan JS. Developments in the characterization of complex rock slope deformation and failure using numerical modelling techniques. Eng Geol 2006;83:217–35.

[26] Yarahmadi Bafghi AR, Verdel T. Sarma-based key-group method for rock slope reliability analyses. Int J Numer Anal Meth Geomech 2005;29:1019–43.

[27] Hack R, Price D, Rengers N. A new approach to rock slope stability—a probability classification (SSPC). Bull Eng Geol Environ 2003;62:167–84 and erratum, p. 185–185.

[28] Yang XL, Li L, Yin JH. Stability analysis of rock slopes with a modified Hoek–Brown failure criterion. Int J Numer Anal Meth Geomech 2004;28:181–90.

[29] Yang XL, Li L, Yin JH. Seismic and static stability analysis for rock slopes by a kinematical approach. Geotechnique 2004;54(8): 543–9.

[30] Yang XL, Zou JF. Stability factors for rock slopes subjected to pore water pressure based on the Hoek–Brown failure criterion. Int J Rock Mech Min Sci 2006;43:1146–52.

[31] Zanbak C. Design charts for rock slopes susceptible to toppling. J Geotech Eng Div ASCE 1983;190(8):1039–62.

[32] Siad L. Seismic stability analysis of fractured rock slopes by yield design theory. Soil Dynam Earthquake Eng 2003;23:203–12.

[33] Marinos V, Marinos P, Hoek E. The geological strength index: applications and limitations. Bull Eng Geol Environ 2005;64: 55–65.

[34] Hoek E. Strength of jointed rock masses. Geotechnique 1983;33(3): 187–223.

[35] Bieniaski ZT. Rock mass classification in rock engineering. In Exploration for rock engineering, Proceedings of the rock mechanics symposium. Balkema: Cape Town; 1976.

[36] Barton N. Some new Q-value correlations to assist in site characterisation and tunnel design. Int J Rock Mech Min Sci 2002; 39(2):185–216.

[37] Hoek E, Rock Engineering. 2000 〈http://www.rocscience.com/hoek/references/Published-Papers.htm〉.

[38] Hoek E, Brown ET. Practical estimates of rock mass strength. Int J Rock Mech Min Sci 1997;34(8):1165–86.

[39] Rocscience, 2D limit equilibrium analysis software, Slide 5.0. 〈www.rocscience.com〉.

[40] Bishop AW. The use of slip circle in stability analysis of slopes. Geotechnique 1955;5(1):7–17.